

Supporting Information for

A Visible-Light and Temperature Responsive Host-Guest System: Photoisomerization of a Ruthenium Complex and Inclusion Complex Formation with Cyclodextrins

Masanari Hirahara,*^a Shota Furutani,^a Hiroki Goto,^b Keiichi Fujimori,^a Takayo, Kawakami-Moriuchi^a

^a Department of Applied Chemistry, Faculty of Engineering, Osaka Institute of Technology, 5-16-1 Omiya, Asahi Ward, Osaka, 535-8585

^b Department of Applied Chemistry, School of Applied Science, National Defense Academy of Japan, 1-10-20 Hashirimizu, Yokosuka, Kanagawa, 239-8686

Supporting Information

Contents

Figure S1— ¹ H NMR spectra of <i>proximal-1</i> during titration experiments with α -CD	S3
Figure S2— ¹ H NMR spectra of <i>proximal-1</i> during titration experiments with β -CD	S4
Figure S3— ¹ H NMR spectra of <i>distal-1</i> during titration experiments with α -CD	S5
Figure S4— ¹ H NMR spectra of <i>distal-1</i> during titration experiments with β -CD	S6
Figure S5— ¹ H NMR spectra of <i>proximal</i> -[Ru(C ₂ tpy)(C ₂ pyqu)OH ₂] ²⁺ during titration experiments with γ -CD	S7
Figure S6— ¹ H NMR spectra of <i>proximal</i> -[Ru(tpy)(C ₁₀ pyqu)OH ₂] ²⁺ during titration experiments with γ -CD	S8
Figure S7—Benesi–Hildebrand plots from ¹ H NMR titration between <i>proximal-1</i> and γ -CD	S9
Figure S8—Benesi–Hildebrand plots from ¹ H NMR titration between <i>proximal-1</i> and β -CD	S10
Figure S9—Benesi–Hildebrand plots from ¹ H NMR titration between <i>proximal-1</i> and α -CD	S11
Figure S10—Benesi–Hildebrand plots from ¹ H NMR titration between <i>proximal</i> -[Ru(C ₂ tpy)(C ₂ pyqu)OH ₂] ²⁺ and γ -CD	S12

Figure S11—Benesi–Hildebrand plots from ^1H NMR titration between <i>proximal</i> -[Ru(tpy)(C ₁₀ pyqu)OH ₂] ²⁺ and γ -CD	S13
Figure S12—Benesi–Hildebrand plots from ^1H NMR titration between <i>distal-1</i> and γ -CD	S14
Figure S13—Benesi–Hildebrand plots from ^1H NMR titration between <i>distal-1</i> and β -CD	S15
Figure S14—Benesi–Hildebrand plots from ^1H NMR titration between <i>distal-1</i> and α -CD	S16
Figure S15— ^1H NMR spectra during thermal back isomerization from <i>distal-1</i> to <i>proximal-1</i> at 293 K	S17
Figure S16—Kinetic traces for thermal back isomerization from <i>distal-1</i> to <i>proximal-1</i> in the absence and presence of γ -CD.	S18
Figure S17—Arrhenius and Eyring plots for thermal-back-isomerization from <i>distal-1</i> to <i>proximal-1</i> .	S19
Figure S18—Kinetic traces for thermal back isomerization at 333K in the presence of cyclodextrins	S20
Table S1—Summary of thermodynamic parameters for thermal-back-isomerization	S21
References	S22

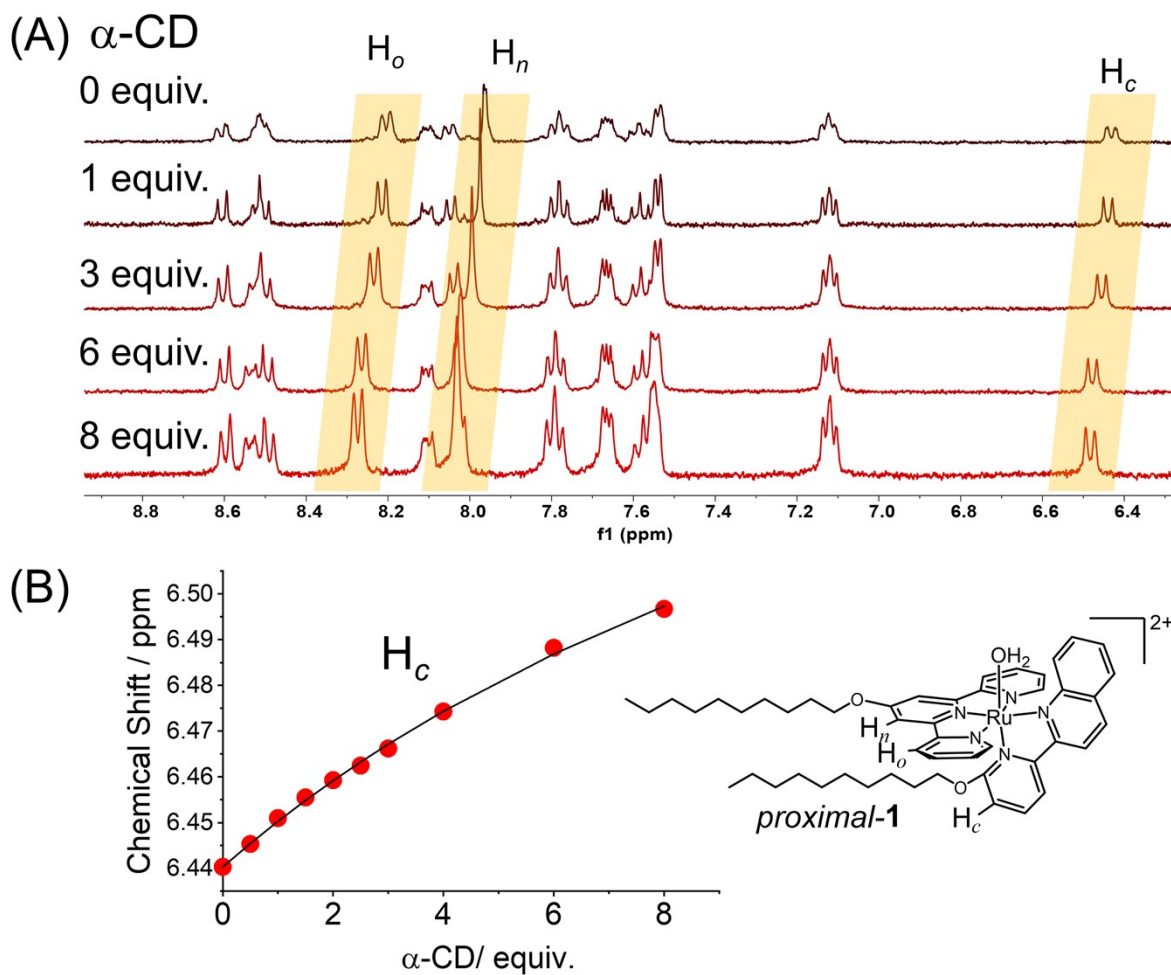


Figure S1. (A) ^1H NMR spectra of *proximal-1* (1.55 mM) during titration experiments with α -CD in D_2O , CD_3OD , and TFE mixed solvent ($v/v/v = 70:40:2$). Peaks of H_o , H_n , and H_c protons are highlighted. (B) Plots of chemical shifts of H_c proton verses equivalents of α -CD.

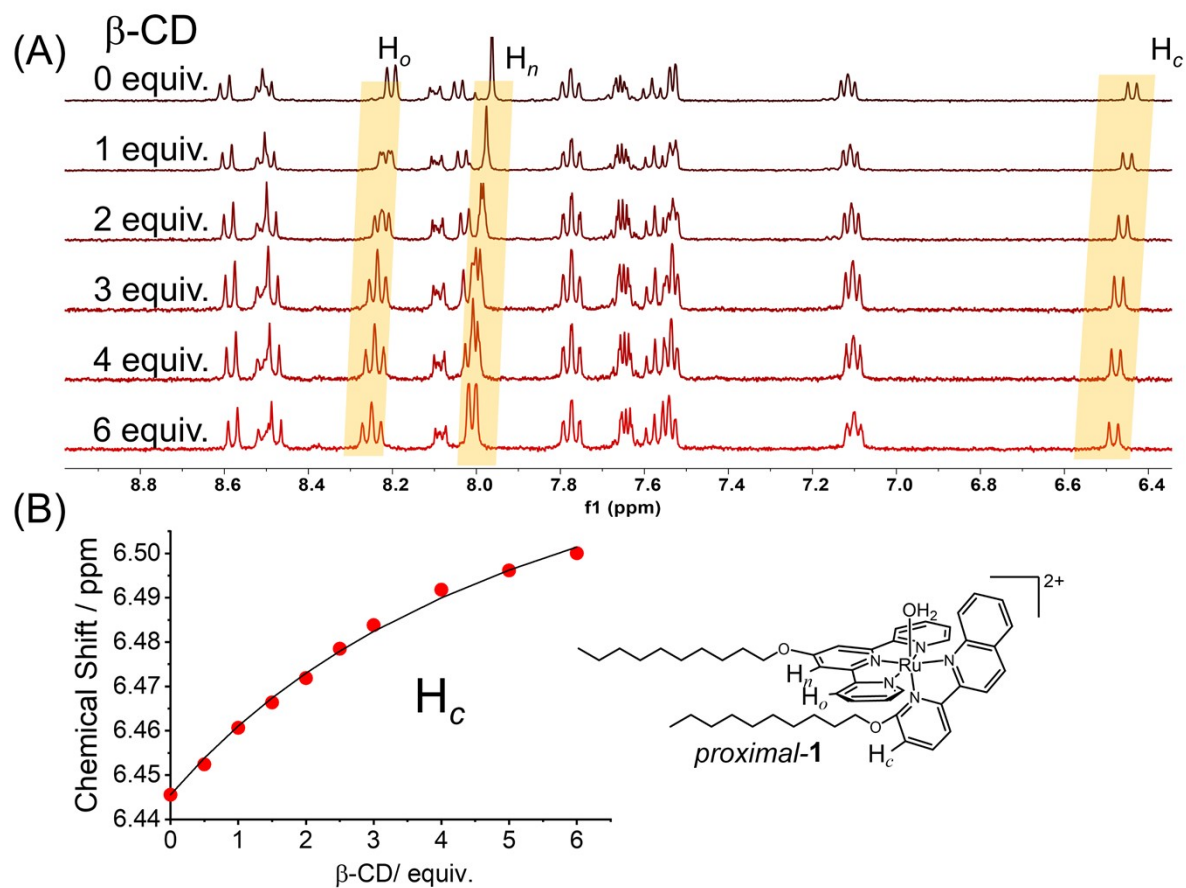


Figure S2. (A) ^1H NMR spectra of *proximal-1* (0.84 mM) during titration experiments with β -CD in D_2O , CD_3OD , and TFE mixed solvent (v/v/v = 70:40:2). Peaks of H_o , H_n , and H_c protons are highlighted. (B) Plots of chemical shifts of H_c proton verses equivalents of β -CD.

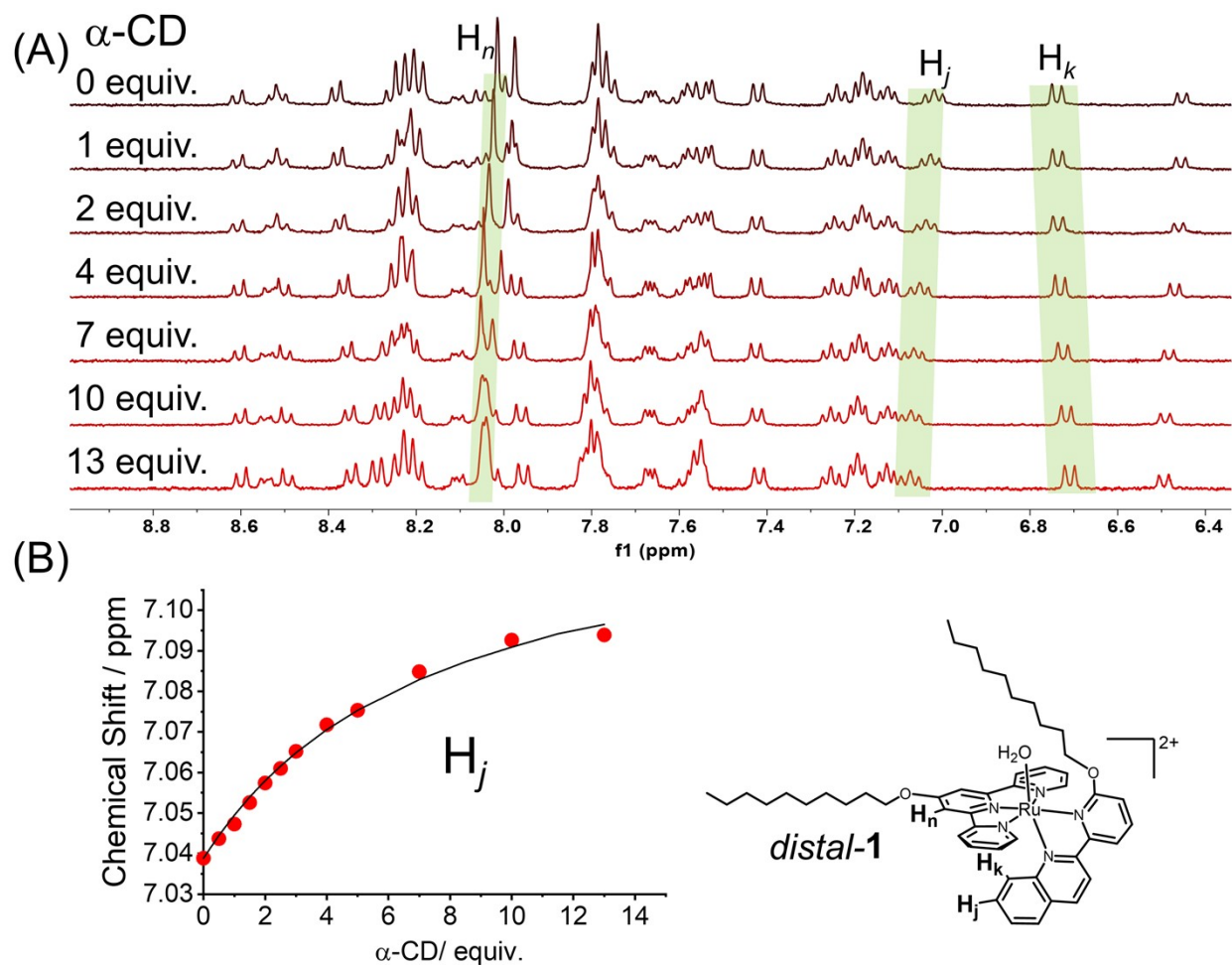


Figure S3. (A) ^1H NMR spectra of *proximal-1* and *distal-1* (total concentration: 1.36 mM, *proximal-1* : *distal-1* = 36 : 64) during titration experiments with α -CD in mixed aqueous solutions (D_2O : CD_3OD : TFE = 70 : 50 : 2). Peaks of H_n , H_j , and H_k protons for *distal-1* are highlighted. (B) Plots of chemical shifts of H_j proton versus equivalents of α -CD.

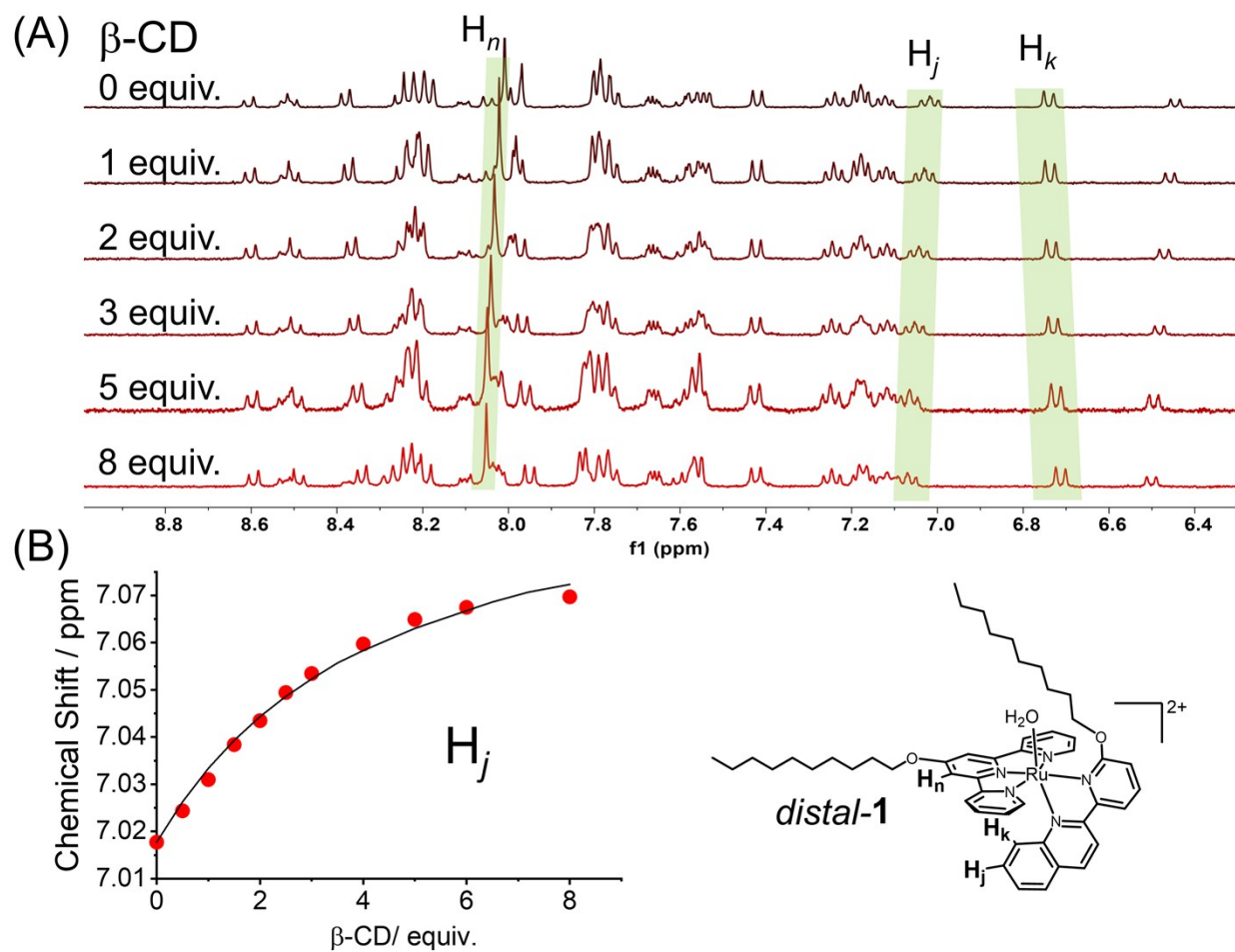


Figure S4. (A) ^1H NMR spectra of *proximal-1* and *distal-1* (total concentration: 0.88 mM, *proximal-1* : *distal-1* = 36 : 64) during titration experiments with β -CD in mixed aqueous solutions (D_2O : CD_3OD : TFE = 70 : 40 : 2). Peaks of H_n , H_j , and H_k protons for *distal-1* are highlighted. (B) Plots of chemical shifts of H_j proton versus equivalents of β -CD, respectively.

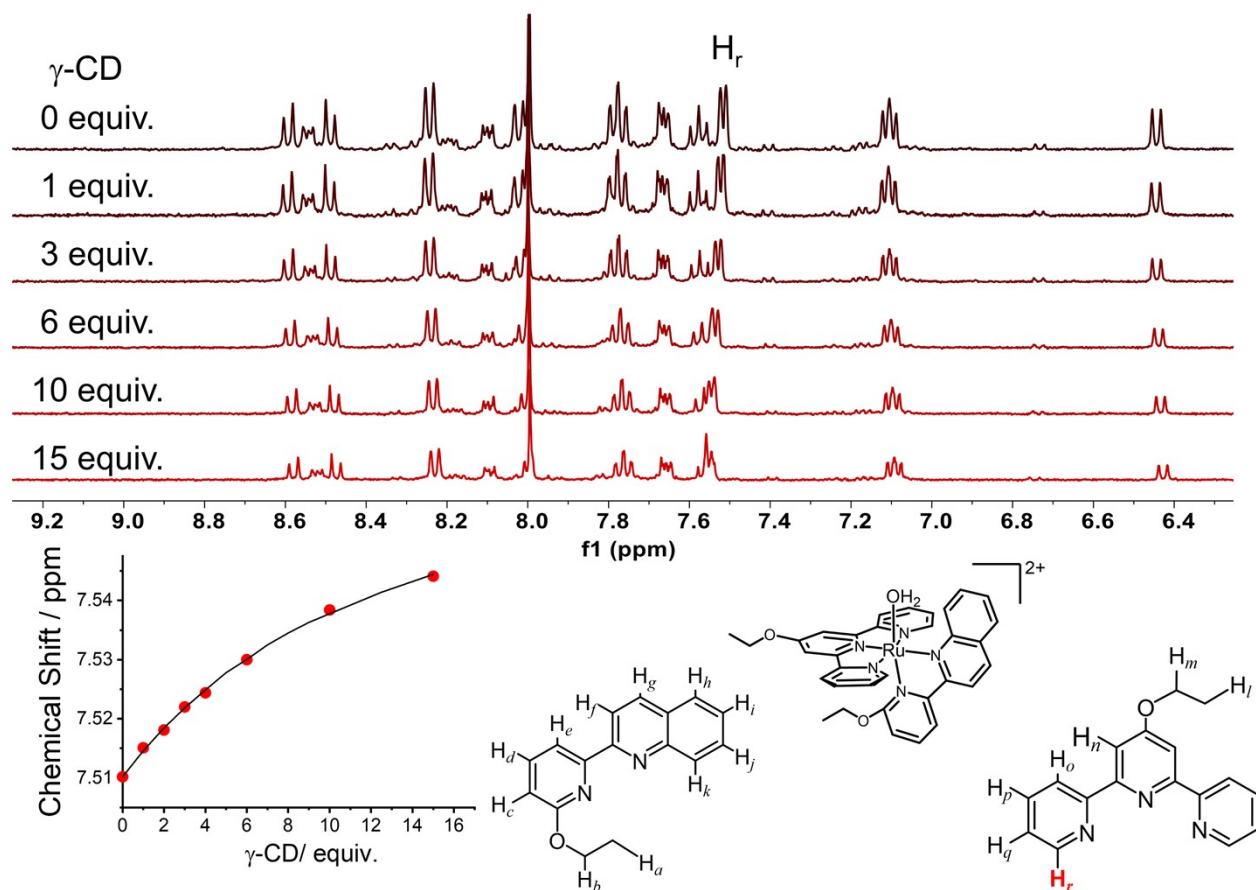


Figure S5. (A) ¹H NMR spectra of proximal-[Ru(C₂tpy)(C₂pyqu)OH₂]²⁺ (1.63 mM) during titration experiments with γ-CD in D₂O, CD₃OD, and TFE mixed solvent (v/v/v = 70:40:2). (B) Plots of chemical shifts of H_r proton versus equivalents of γ-CD. Small peaks correspond to distal-[Ru(C₂tpy)(C₂pyqu)OH₂]²⁺.¹

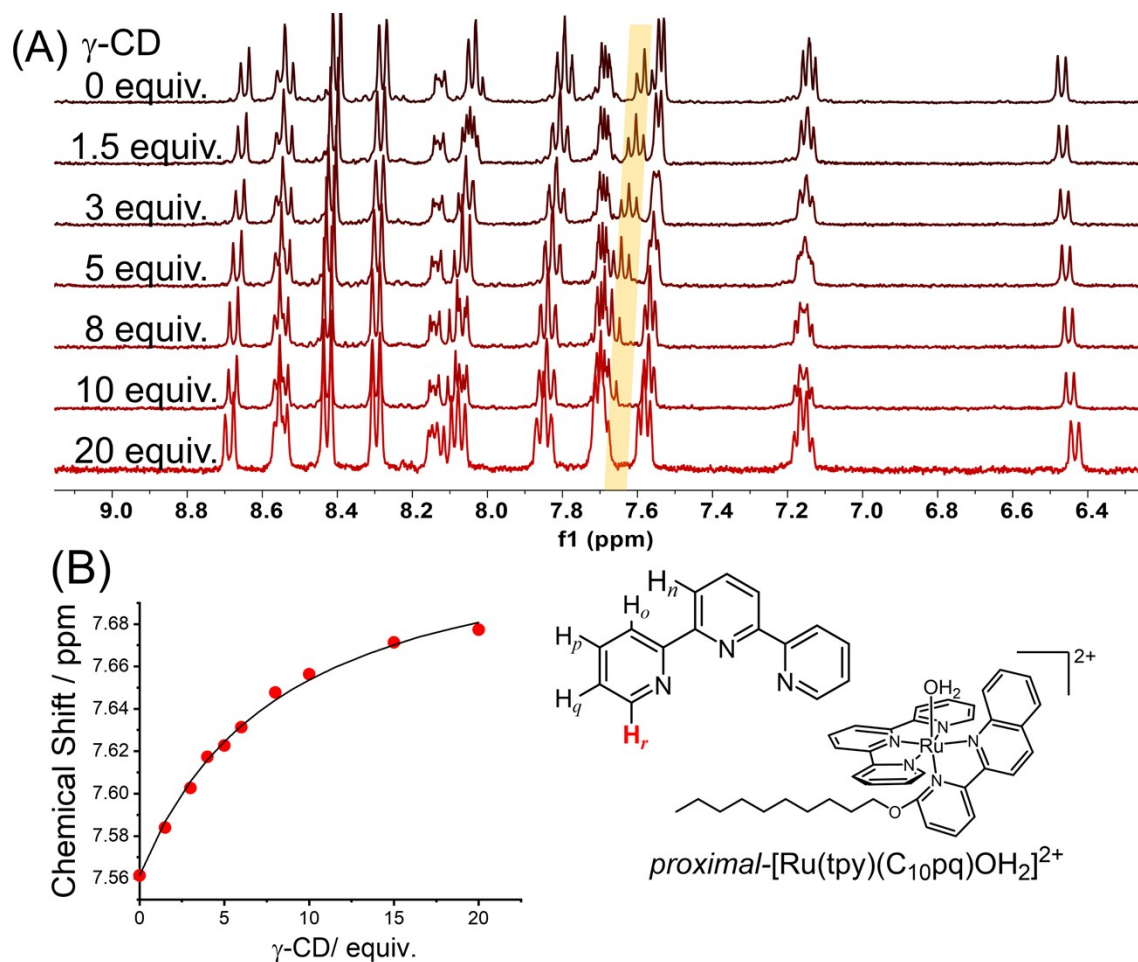


Figure S6. (A) ^1H NMR spectra of *proximal*-[Ru(tpy)(C₁₀pyqu)OH₂]²⁺ (1.58 mM) during titration experiments with γ -CD in D₂O, CD₃OD, and TFE mixed solvent (v/v/v = 70:40:2). (B) Plots of chemical shifts of H_r proton versus equivalents of γ -CD.

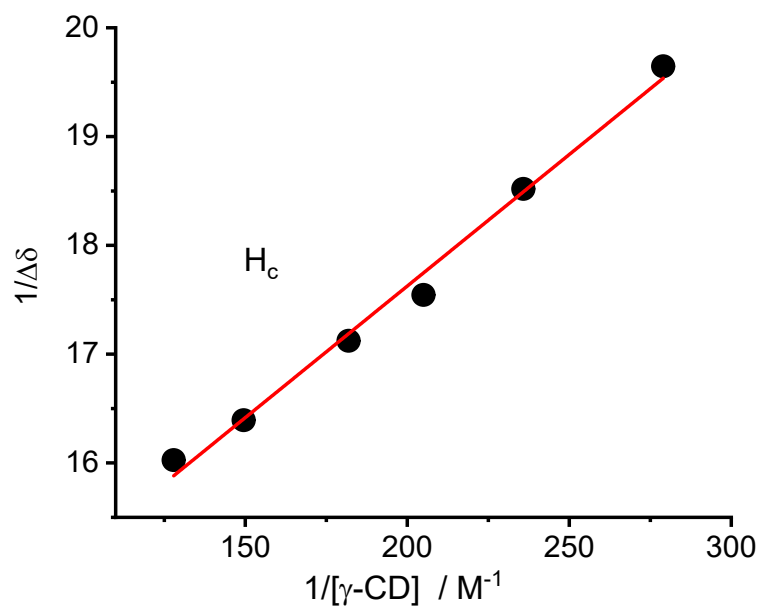


Figure S7. Benesi–Hildebrand plots from ^1H NMR titration between *proximal-1* and $\gamma\text{-CD}$.

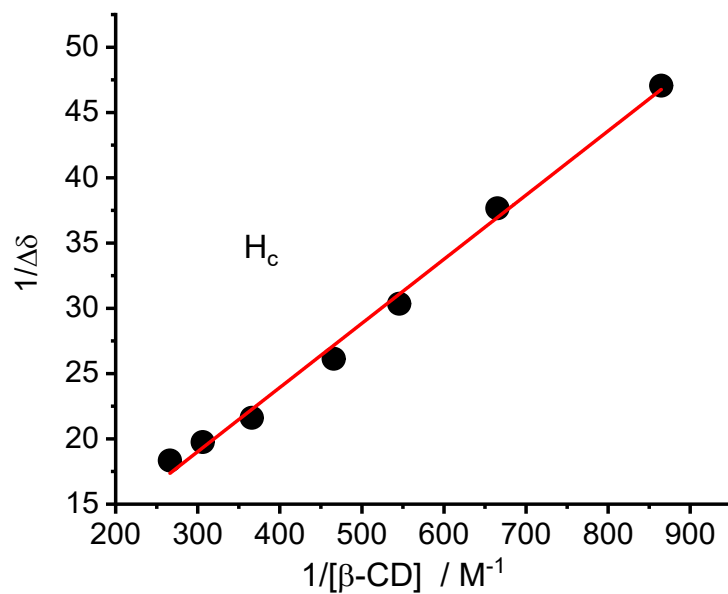


Figure S8. Benesi–Hildebrand plots from ^1H NMR titration between *proximal-1* and $\beta\text{-CD}$.

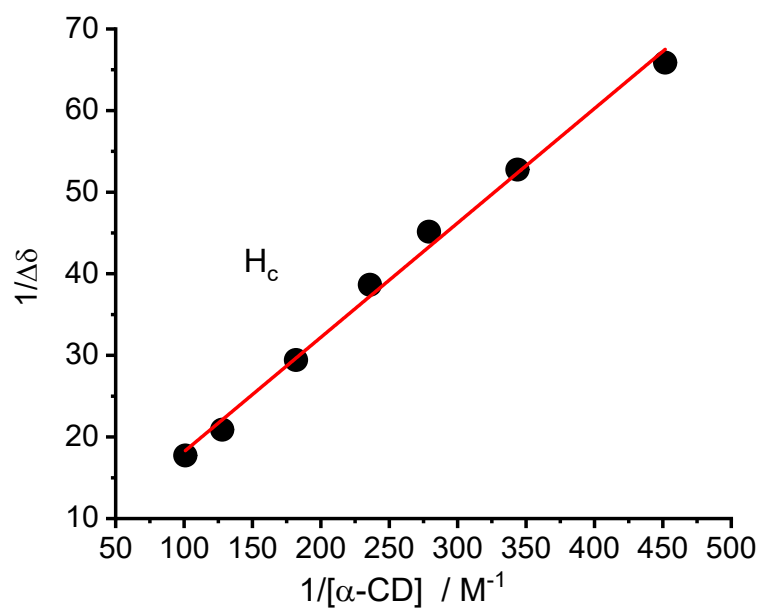


Figure S9. Benesi–Hildebrand plots from ^1H NMR titration between *proximal-1* and $\alpha\text{-CD}$.

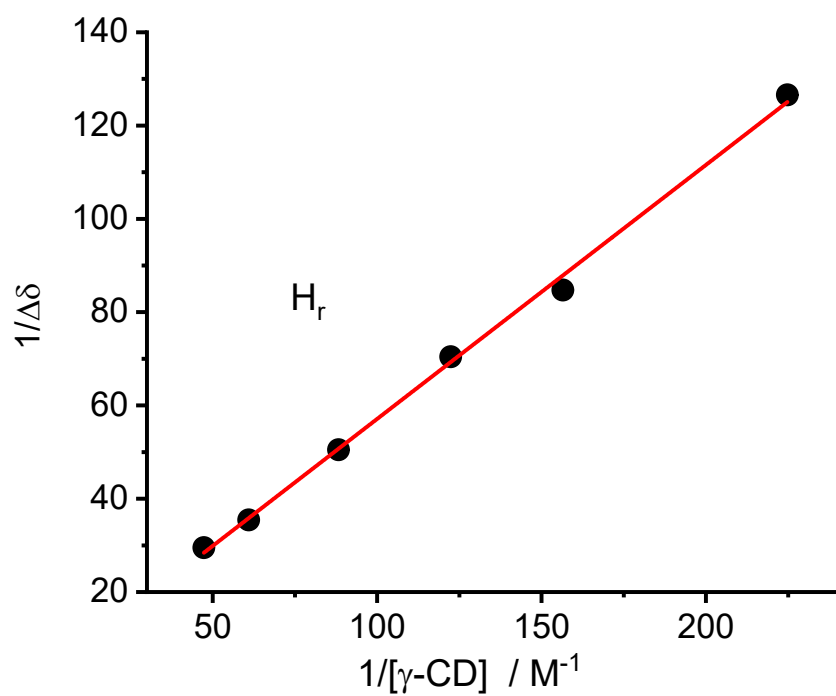


Figure S10. Benesi-Hildebrand plots from ^1H NMR titration between *proximal*- $[\text{Ru}(\text{C}_2\text{tpy})(\text{C}_2\text{pyqu})\text{OH}_2]^{2+}$ and γ -CD.

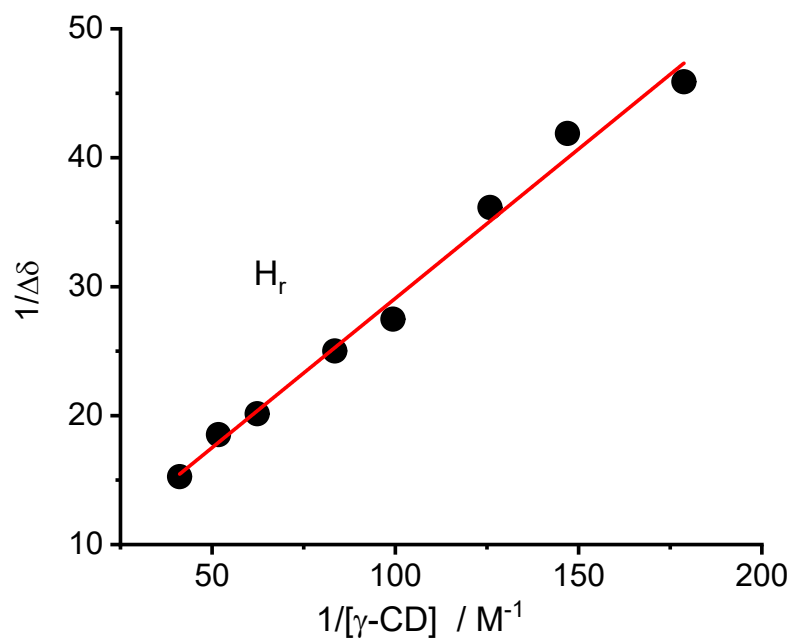


Figure S11. Benesi–Hildebrand plots from ^1H NMR titration between *proximal*- $[\text{Ru}(\text{tpy})(\text{C}_{10}\text{pyqu})\text{OH}_2]^{2+}$ and $\gamma\text{-CD}$.

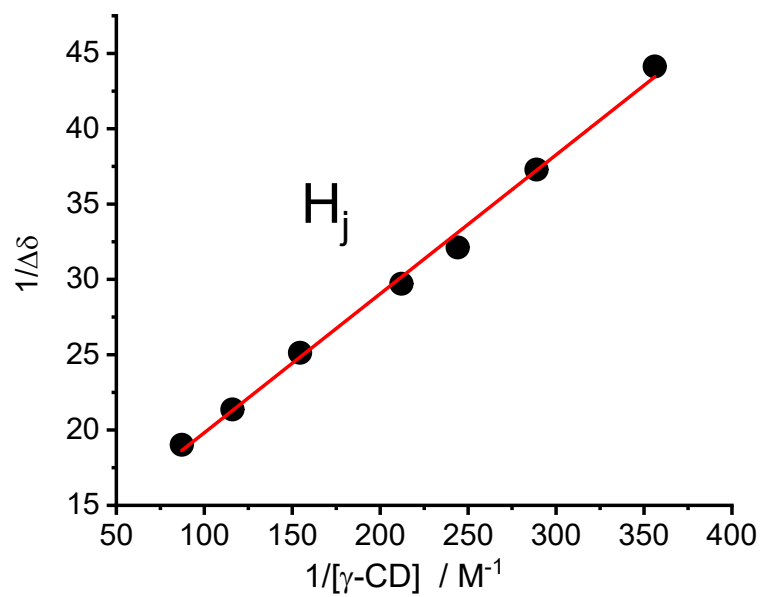


Figure S12. Benesi-Hildebrand plots from ^1H NMR titration between *distal-1* and $\gamma\text{-CD}$.

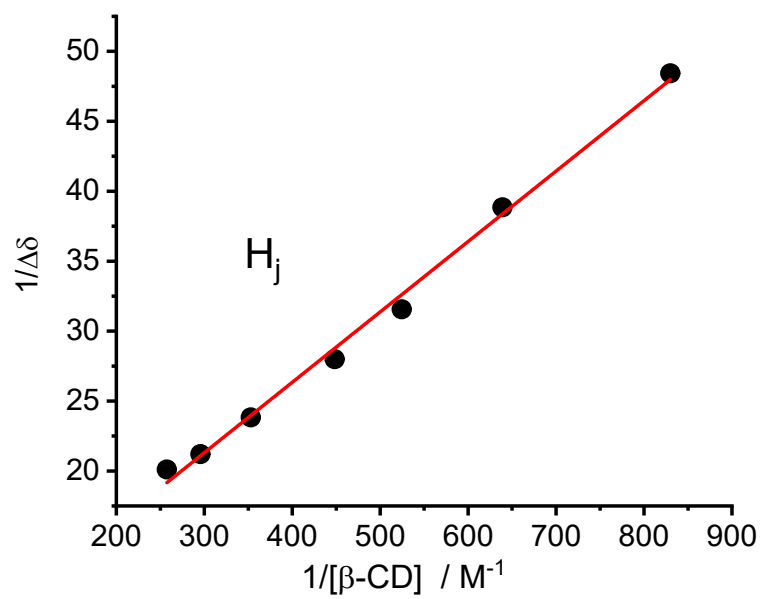


Figure S13. Benesi-Hildebrand plots from ^1H NMR titration between *distal-1* and $\beta\text{-CD}$.

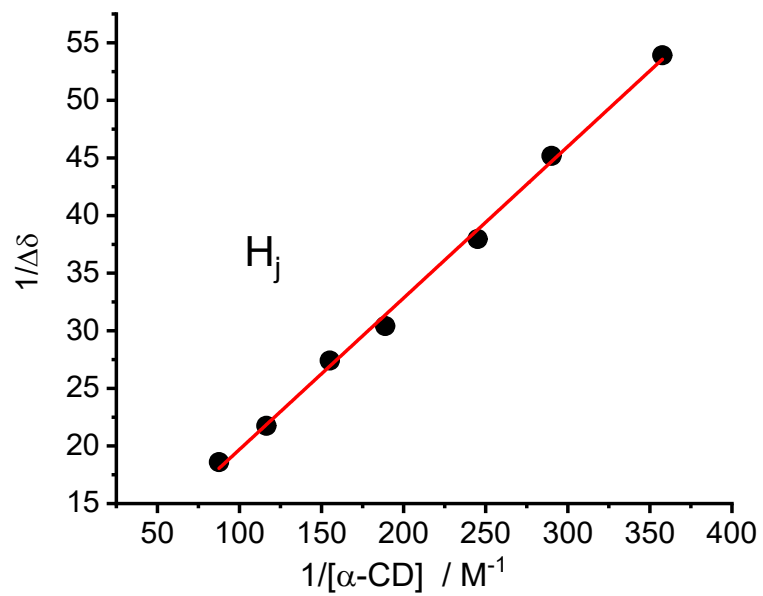


Figure S14. Benesi-Hildebrand plots from ^1H NMR titration between *distal-1* and $\alpha\text{-CD}$.

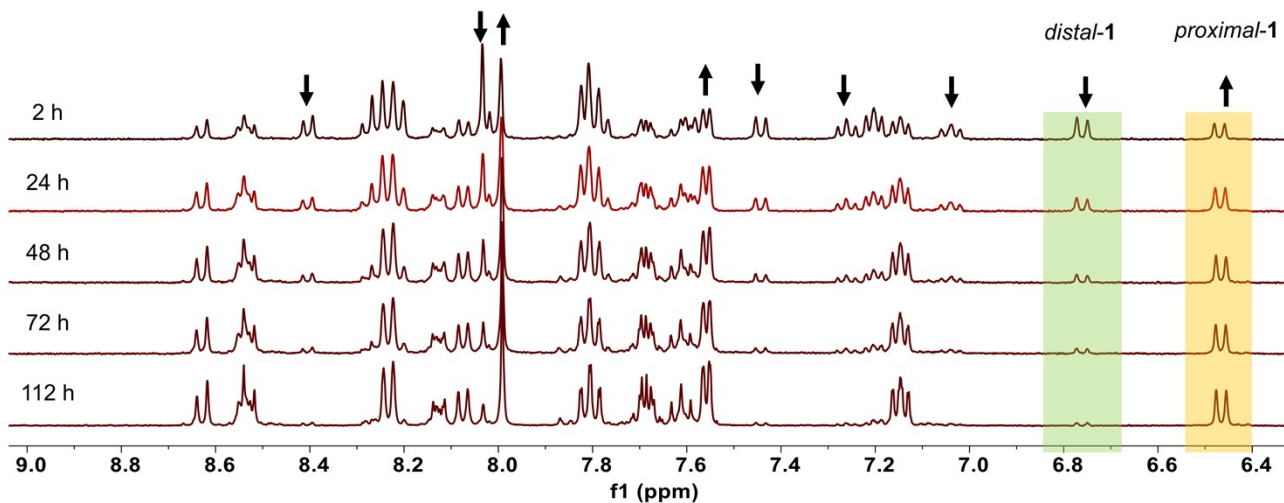


Figure S15. ¹H NMR spectra during thermal back isomerization from *distal-1* to *proximal-1* at 293 K. The sample solution was prepared by light irradiation to an aqueous solution of *proximal-1* (1.5 mM) in mixed aqueous solution (D₂O : CD₃OD : TFE = 70 : 50 : 2). H_k proton of *distal-1* and H_c proton of *proximal-1* were highlighted with green and orange, respectively. The progress of the reaction was monitored in the dark.

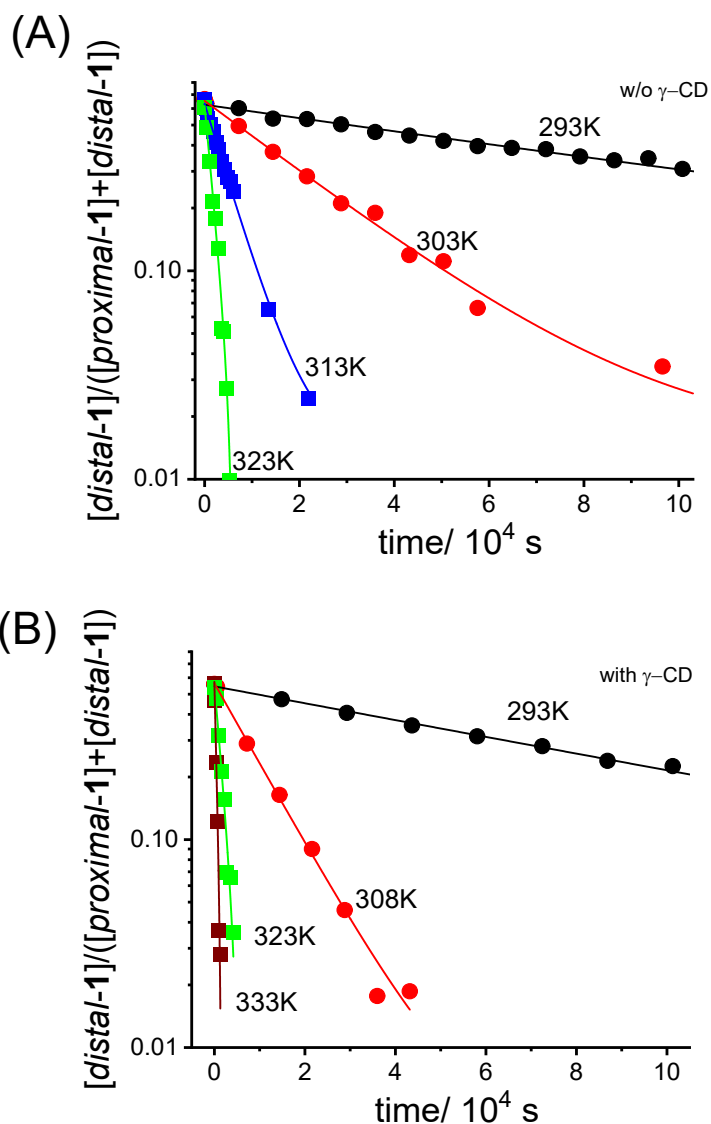


Figure S16. Kinetic traces for thermal back isomerization from *distal-1* to *proximal-1* at various temperatures. (A) Traces at 293, 303, 313, and 323 K in the absence of a host molecule. (B) Traces at 293, 308, 323, and 333 K in the presence of 5 equiv. of γ -CD. The concentration of *distal-1* was estimated based on the integration of an H_c proton for *proximal-1* and an H_k proton for *distal-1*, respectively.

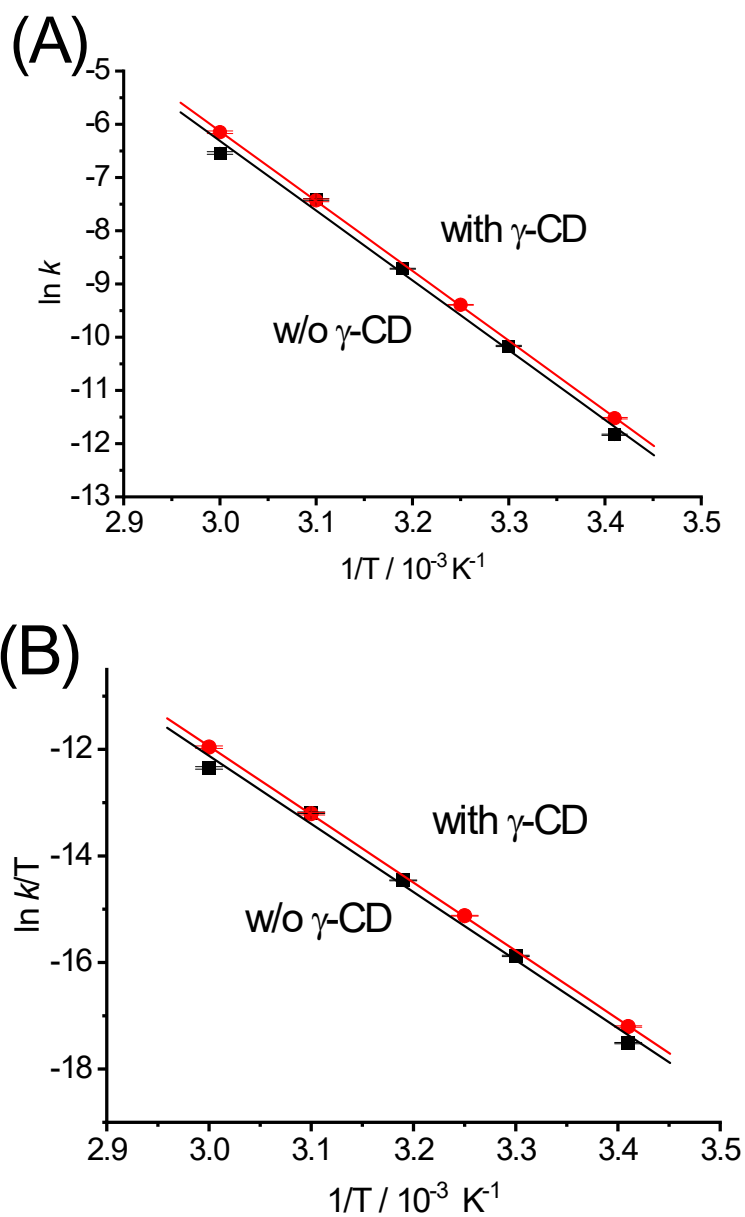


Figure S17. (A) Arrhenius and (B) Eyring plots for the thermal-back-isomerization from *distal-1* to *proximal-1*. Plots for the isomerization in the absence and presence of γ -CD are plotted with black square and red circle, respectively.

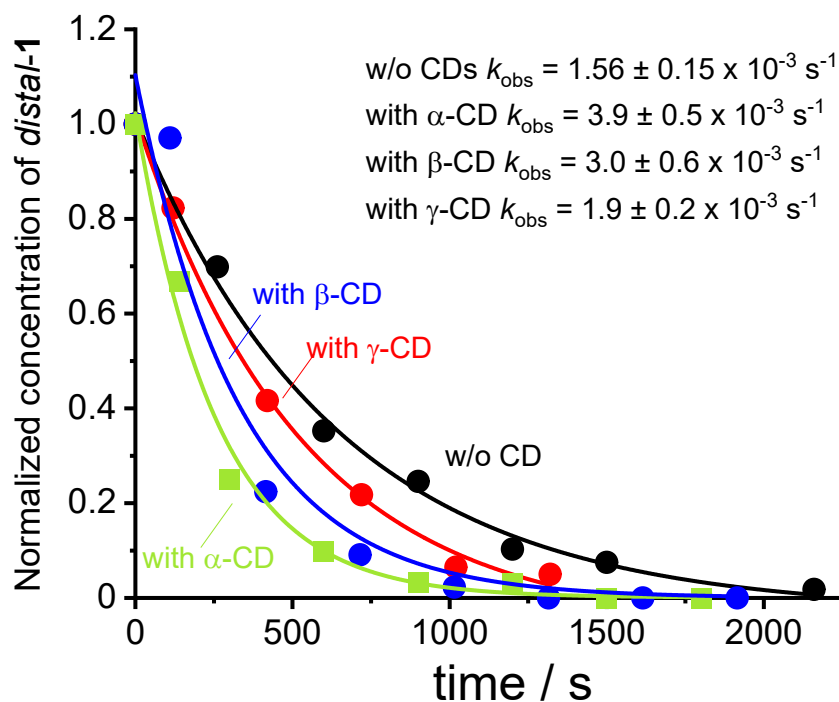


Figure S18. Kinetic traces for thermal back isomerization from *distal-1* to *proximal-1* at 333K in the absence or presence of cyclodextrins. The sample solution of *distal-1* and *proximal-1* in the photostationary state was prepared by light irradiation to an aqueous solution of *proximal-1* in the mixed aqueous solution (D₂O : CD₃OD : TFE = 70 : 50 : 2) prior to the measurements. Black: in the absence of cyclodextrins ($c_{Ru} = 1.52$ mM), red: in the presence of γ -CD ($c_{Ru} = 1.38$ mM, $[\gamma\text{-CD}] = 7.1$ mM), blue; in the presence of β -CD ($c_{Ru} = 0.70$ mM, $[\beta\text{-CD}] = 3.5$ mM), and green; in the presence of α -CD ($c_{Ru} = 1.35$ mM, $[\alpha\text{-CD}] = 6.35$ mM). The initial concentration was normalized for comparison. $c_{Ru} = [proximal-1] + [distal-1]$.

Table S1. Summary of thermodynamic parameters for thermal-back-isomerization from *distal-1* to *proximal-1* in the absence and presence of γ -CD (5 equiv.)

	$E_{\text{act}} / \text{kJ mol}^{-1}$	$\Delta H^{\ddagger} / \text{kJ mol}^{-1}$	$\Delta S^{\ddagger} / \text{J mol}^{-1} \text{K}^{-1}$	$\Delta G^{\ddagger} / \text{kJ mol}^{-1}$
With γ -CD	109 ± 1	106 ± 1	22 ± 2	99 ± 1
w/o γ -CD	109 ± 5	106 ± 5	21 ± 17	100 ± 7

References

1. Hirahara, M.; Goto, H.; Yagi, M.; Umemura, Y., A multi-stimuli responsive ruthenium complex for catalytic water oxidation. *Chem. Commun.* **2020**, 56 (84), 12825-12828.